

PACS numbers: 42.55.Ks; 33.50.–j; 82.50.–m
DOI: 10.1070/QE2011v041n02ABEH014431

Kinetics of $O_2(^1\Sigma)$ formation in the reaction $O_2(^1\Delta) + O_2(^1\Delta) \rightarrow O_2(^1\Sigma) + O_2(^3\Sigma)$

M.V. Zagidullin, N.A. Khvatov, A.Yu. Nyagashkin

Abstract. **The dependence of the ratio of specific powers of dimole radiation of singlet oxygen in the 634 nm band and in the b–X band of the $O_2(^1\Sigma)$ molecule in the $O_2(X)–O_2(^1\Delta)–O_2(^1\Sigma)–H_2O–CO_2$ mixture on the CO_2 concentration is measured. As a result, the rate constant of the reaction $O_2(^1\Delta) + O_2(^1\Delta) \rightarrow O_2(^1\Sigma) + O_2(^3\Sigma)$ at the temperature ~330 K is found to equal $(4.5 \pm 1.1)\times10^{-17}$ cm^3 s^{-1}.**

Keywords: *oxygen–iodine laser, dimole radiation, singlet oxygen, pulling reaction.*

1. Introduction

Gas phase reactions involving singlet oxygen $O_2(a^1\Delta)$ are of interest in the studies of atmosphere physics [1], electric discharge in oxygen [2], and kinetics of chemical oxygen–iodine laser [3]. In particular, attention is attracted by the process of collision of two molecules $O_2(a)$ that yields oxygen molecules in the ground ($X^3\Sigma$) and the second excited electron ($b^1\Sigma$) states (pulling reaction):

$$O_2(a) + O_2(a) \rightarrow O_2(b) + O_2(X). \quad (1)$$

In the chemical oxygen–iodine laser the source of the $O_2(a)$ molecules is a chemical gas singlet oxygen generator (SOG), based on the reaction between chlorine and alkaline solution of hydrogen peroxide. The gain in the active medium of the oxygen–iodine laser is implemented using the transition $^2P_{1/2}–^2P_{3/2}$ in the iodine atom that appears when mixing the molecular iodine with singlet oxygen. In correspondence with some kinetic models, the process of atomic iodine formation in the active medium of the oxygen–iodine laser starts with the reaction $O_2(b) + I_2 \rightarrow O_2(X) + 2I$ [4, 5], the rate of which is proportional to the concentration of $O_2(b)$ molecules. On reaching a certain critical concentration of the iodine atoms in this reaction [5] and, possibly, in other initiating reactions [4], a chain process of molecular iodine dissociation begins, in which the iodine atoms play an active role. The steady-state concentration of $O_2(b)$ molecules at the SOG output is

$$n_b = k_1 n_a^2 / K_b, \quad (2)$$

where k_1 is the rate constant of reaction (1); K_b is the total probability of $O_2(b)$ loss as a result of homogeneous and heterogeneous processes; n_a, n_b is the concentration of the oxygen molecules $O_2(a)$ and $O_2(b)$. The values of k_1 obtained earlier at room temperature were $\sim2\times10^{-17}$ cm^3 s^{-1} [2, 6] and $(2.7\pm0.4)\times10^{-17}$ cm^3 s^{-1} [7]. The temperature dependence of k_1 was studied in [8, 9]. According to theoretical estimations, $k_1 \approx 10^{-16}$ cm^3 s^{-1} [10] and 10^{-17} cm^3 s^{-1} [11]. Under the conditions when (2) is valid, the determination of k_1 is reduced to the measurements of K_b, n_a, and n_b [2, 6, 7]. Systematic errors of these measurements affect the accuracy of the determination of k_1.

In the present paper we measure the ratio of specific powers of the dimole radiation of the molecule $O_2(a)$ and the b–X band radiation of the molecule $O_2(b)$ in the mixture $O_2(X)–O_2(a)–O_2(b)–H_2O–CO_2$, proportional to the ratio n_a^2/n_b. Under the conditions, when the CO_2 molecule is a predominant quencher of the $O_2(b)$ molecule, the value of k_1 is determined using (2). In the experiments we used the gas mixture $O_2(X)–O_2(a)–O_2(b)–H_2O–CO_2$ with large enough concentration of $O_2(a)$, small content of H_2O and controlled concentration of CO_2.

2. Experiment and measurements

A schematic diagram of the experimental setup is presented in Fig. 1. The gas mixture $O_2(X)–O_2(a)–H_2O$ was created as a result of the reaction of chlorine flow with streams of alkaline solution of the hydrogen peroxide in a stream SOG [12]. Then the gas flow of $O_2(X)–O_2(a)–H_2O$ passed through a water vapour trap (WVT), having the temperature of about –90 °C, and entered the optical diagnostic unit (ODU). The gas trans-

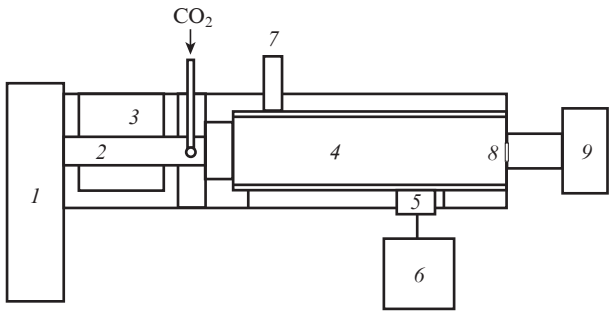

Figure 1. Schematic diagram of the experimental setup:
(*1*) SOG; (*2*) WVT; (*3*) a bath with ethanol at the temperature –90 °C; (*4*) ODU; (*5*) carriage; (*6*) AvaSpec-3648 spectrometer; (*7*) germanium detector; (*8*) choke orifice; (*9*) forepump.

M.V. Zagidullin, N.A. Khvatov, A.Yu. Nyagashkin Samara Branch of P.N. Lebedev Physics Institute, Russian Academy of Sciences, Novo-Sadovaya ul. 221, 443011 Samara, Russia;
e-mail: marsel@fian.smr.ru

Received 9 September 2010; revision received 11 November 2010
Kvantovaya Elektronika **41** (2) 135–138 (2011)
Translated by V.L. Derbov

port of the ODU was a rectangular channel 25 mm high, 8 mm wide and 120 mm long. The side walls of the ODU were made of fluoroplastic, the top and bottom walls were made of 2.5-mm-thick quartz. Between the WVT and the ODU the carbon dioxide gas was admixed to the $O_2(X)-O_2(a)-H_2O$ flow. The radiation of the gas mixture $O_2(X)-O_2(a)-H_2O-CO_2$ from ODU in the wavelength range 600–800 nm was registered by means of the AvaSpec-3648 optical fibre spectrometer (Avantes, Holland) with a CCD detector array. The input end of the optical fibre was placed closely to the quartz wall in the middle between the fluoroplastic walls and was mounted on a carriage that could move along the ODU. The optical fibre spectrometer system captured the radiation of only those molecules that were located in the ODU within the cone with the angle 15° and the vertex at the input end of the fibre. The spectra of dimole radiation (DR) (0,0–0,0) $O_2(a,0) + O_2(a,0) \rightarrow O_2(X,0) + O_2(X,0) + h\nu$ (λ = 634 nm) and radiation in the b–X(0–0) band (λ = 762 nm) of $O_2(b)$ molecules were registered simultaneously. The absolute spectral sensitivity $R(\lambda)$ of the spectrometer was certified by its manufacturer to 9.5% within the whole spectral region 600–800 nm. In addition to the absolute calibration, the relative spectral sensitivity $r(\lambda)$ of the optical fibre–spectrometer–CCD array system was measured using the radiation of a tungsten lamp with the colour temperature 2850 K. The ratio $R(\lambda)/r(\lambda)$ appeared to be constant in the wavelength range 600–800 nm to 2%. Therefore, we assume that for any wavelengths λ_1, λ_2 in the region 600–800 nm the ratio $r(\lambda_1)/r(\lambda_2)$ is known to not worse than 4%.

The specific spectral radiation power from the gas volume was determined using the formula $i(\lambda)$[phot. cm^{-3} s^{-1} nm^{-1}] = $4t^{-1}L^{-1}\varepsilon^{-1}C(\lambda)R(\lambda)$, where $C(\lambda)$ is the number of counts of a CCD array pixel; L =2.5 cm is the ODU height; $\varepsilon \approx 0.93$ is the quartz wall transmission; t is the spectra exposure time. The specific powers in the b–X(0–0) and DR(0,0–0,0) bands were found using the expressions

$$I_b = A_b n_b = \int_{b-X} i(\lambda)\mathrm{d}\lambda, \quad I_D = k_D n_a^2 = \int_{DE} i(\lambda)\mathrm{d}\lambda, \qquad (3)$$

where A_b is the Einstein coefficient for the transition b–X(0–0); k_D is the rate constant of the DR. The integrals in (3) are taken over the corresponding spectral band. The gas temperature in the ODU was determined using the partially resolved rotational structure of the spectrum of the b–X(0–0) band, or the width of the dimole radiation spectrum, as described, e.g., in [13]. A germanium photodetector, placed at 5 cm from the point of CO_2 admixture, registered the radiation of the a–X band of oxygen $O_2(a)$ molecules.

The gas evacuation from the ODU was implemented through the delivery outlet using a forepump with volumetric capacity 5 L s^{-1}, independent of the gas pressure in the limits of the present experiment. Before entering the pump the gas temperature was equal to that of the walls of the gas-flow tract, namely, ~295 K. Therefore, the pressure at the pump input was directly proportional to the molar flow rate of the gas through the ODU. The pressure values in the ODU an at the pump input were measured with the error of 1.5%.

3. Experimental results and discussion

The chlorine flow rate in the experiments was ~0.8 mmol s^{-1}, the efficiency of its utilisation exceeding 97%. A few seconds after the start of the SOG, when the steady-state values were achieved by the gas pressure over the whole gas-flow tract and by the response of the germanium photodetector, CO_2 was admixed to the flow of $O_2(X)-O_2(a)-H_2O$. After the secondary stabilisation of the flow parameters the scanning of the radiation spectra was started during the exposure time equal to t = 5 s. After that the chlorine supply to the SOG was terminated and the pressure in the flow of pure CO_2 was measured before the forepump. The CO_2 concentration in the mixture $O_2(X)-O_2(a)-H_2O-CO_2$ was found using the formula

$$n_{CO_2} = \frac{p_{CO_2}}{p}\frac{p_{ODS}}{k_B T},$$

where p, p_{CO_2} are the pressure values in the flow of $O_2(X)-O_2(a)-H_2O-CO_2$ and in the flow of pure CO_2 before the entrance of the forepump; p_{ODS} and T are the pressure and the temperature in the flow of $O_2(X)-O_2(a)-H_2O-CO_2$ in the ODU; k_B is the Boltzmann constant. The present calculation of n_{CO_2} is valid under the condition of complete mixing of the CO_2 flow with the flow of $O_2(X)-O_2(a)-H_2O$.

Figure 2 presents typical spectra, obtained in the case when the carriage is at the distance of 11 cm from the CO_2 admixture point, the concentration of n_{CO_2} is 3.8×10^{16} cm^3 s^{-1}, the total gas pressure is 15 Torr, and its temperature is ~320 K. Using $k_D = 6\times10^{-23}$ cm^3 s^{-1} [14], $A_b = 8.8\times10^{-2}$ s^{-1} [15] and (3) in the present experiment, the following concentration values were obtained: $n_a \approx 10^{17}$ cm^{-3}, $n_b \approx 2.5\times10^{13}$ cm^{-3}.

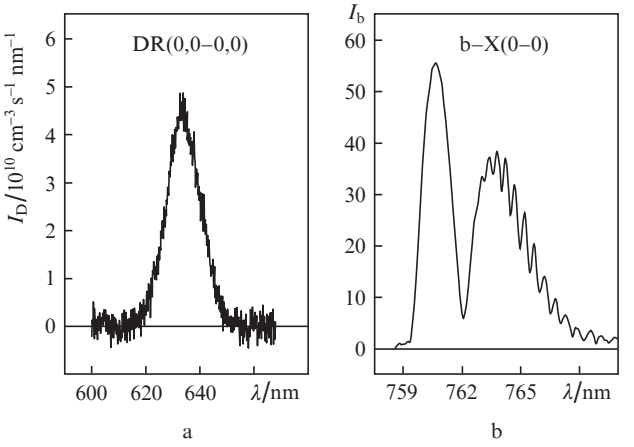

Figure 2. Emission spectra of specific power of the gas mixture $O_2(a)-O_2(b)-O_2(X)-CO_2$ in the band of dimole radiation (0,0–0,0) (a) and in the band b–X(0–0) at $n_a \approx 10^{17}$ cm^{-3}, $n_b \approx 2.5\times10^{13}$ cm^{-3}, n_{CO_2} = 3.8×10^{16} cm^{-3}, the total gas pressure 15 Torr and the temperature 320 ± 5 K.

According to (2) and (3),

$$\frac{I_D}{I_b} = \frac{k_D n_a^2}{A_b n_b} = \frac{k_D}{k_1 A_b} K_b, \qquad (4)$$

where $K_b = K + k_{CO_2} n_{CO_2}$; k_{CO_2} is the rate constant of the quenching reaction $O_2(b) + CO_2 \rightarrow O_2(X) + CO_2$; K is the total probability of $O_2(b)$ deactivation at the wall and other molecules (O_2, H_2O, Cl_2). It was found, that both I_D and I_b decrease with the growth of the distance from the CO_2 admixture point in the range 5–11 cm; however, at fixed consumption of CO_2 the ratio (4) remains constant within ~6%. Variation in the CO_2 concentration in the flow $O_2(X)-O_2(a)-$

H_2O-CO_2 was implemented via changing its flow rate or the cross section of the choke orifice at the ODU output. The dependence of I_D/I_b on n_{CO_2} is illustrated in Fig. 3, where only those experiments are presented, in which the gas temperature at the distance 11 cm from the CO_2 admixture point was within the limits of 320–340 K. The independence of the ratio I_D/I_b of the carriage position and its linear dependence on n_{CO_2} evidence in favour of practically complete mixing of the CO_2 flow with the flow $O_2(X)-O_2(a)-H_2O$ at the distance of 11 cm from the CO_2 admixture point in the chosen experiments. At $n_{CO_2} = 0$ the ratio $I_D/I_b \approx 0.05$. The linear approximation of the $I_D/I_b(n_{CO_2})$ dependence, presented in Fig. 3, yields

$$\frac{k_D k_{CO_2}}{k_1 A_b} = (7.8 \pm 0.2)\times 10^{-18}\ \text{cm}^3.$$

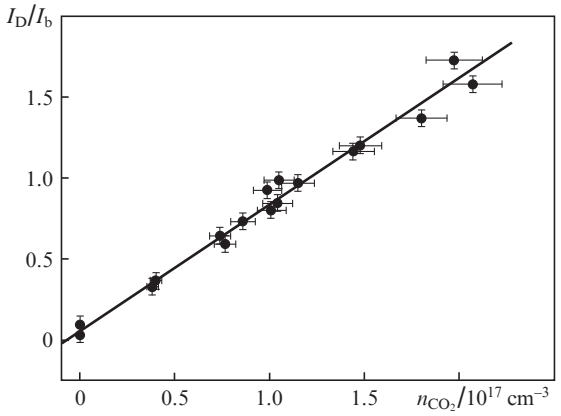

Figure 3. The ratio of specific powers of dimole radiation and radiation in the b–X(0–0) band versus the concentration of the carbon dioxide gas. The distance between the point of CO_2 admixture and the point of spectra recording is 11 cm.

Taking into account the errors in measuring temperature (±10K), pressure (1.5%), and ratio of spectral sensitivities (4%), we get

$$\frac{k_D k_{CO_2}}{k_1 A_b} = (7.8 \pm 0.8)\times 10^{-18}\ \text{cm}^3. \qquad (5)$$

The estimate of k_1 depends on the choice of the numerical values of the radiation constants A_b, k_D and the rate constant k_{CO_2} of quenching $O_2(b)$ by the CO_2 molecules. The most reliable value of k_D, equal to $(6.1\pm0.3)\times10^{-23}$ cm^3 s^{-1}, is derived from the value of the integral dimole absorption of oxygen [16, 17]. The largest disagreement in the literature data relates the rate constant k_{CO_2}, namely, $(3\pm1)\times10^{-13}$ cm^3 s^{-1} [18], $(3.48\pm0.47)\times10^{-13}$ cm^3 s^{-1} [19], $(5\pm0.3)\times10^{-13}$ cm^3 s^{-1} [20], $(4.6\pm0.5)\times10^{-13}$ cm^3 s^{-1} [21], $(4.53\pm0.29)\times10^{-13}$ cm^3 s^{-1} [22], $(6.1\pm0.5)\times10^{-13}$ cm^3 s^{-1} [23]. In our opinion, the most reliable are the values of k_{CO_2} obtained in [20–23], where it was determined by directs measurement of the probability of $O_2(b)$ loss in the process $O_2(b) + CO_2 \rightarrow O_2(X) + CO_2$. According to the latest data, $A_b = (8.69\pm0.03)\times10^{-2}$ s^{-1} [24], which differs only slightly from the value 8.8×10^{-2} s^{-1}, given in the HITRAN database [15]. Therefore, substituting $k_D = (6.1\pm0.3)\times10^{-23}$ cm^3 s^{-1}, $A_b = (8.69\pm0.03)\times10^{-2}$ s^{-1} and $k_{CO_2} = (5\pm0.5)\times10^{-13}$ cm^3 s^{-1} into (5), we get $k_1 = (4.5\pm1.1)\times10^{-17}$ cm^3 s^{-1} for the temperature ~330 K. Using the temperature dependence of k_1, described in [8], we have $k_1 = (4.0\pm1)\times10^{-17}$ cm^3 s^{-1} at the temperature 300 K. This is about two times greater than the k_1 values, obtained in [2, 6]. Within the error this estimate of k_1 is close to $(2.7\pm0.4)\times10^{-17}$ cm^3 s^{-1} from [7].

Only the ratio of relative spectral sensitivities of the spectrometer and the calculation of the CO_2 concentration in the $O_2(X)-O_2(a)-H_2O-CO_2$ flow were used for calculating the numerical value of (5). We see no reasons why they could be determined with systematic error of ~100%, which could explain the discrepancy with the results of [2, 6]. It seems to us, that the smaller values of $k_1 \approx 2\times10^{-17}$ cm^3 s^{-1}, obtained in these papers, are due to systematic errors in the determination of the absolute concentration of the $O_2(a)$ and $O_2(b)$ molecules and to insufficient account for the deactivation of $O_2(b)$ at a wall, as pointed out in [25].

Reaction (1) followed by the reaction $O_2(b) + M \rightarrow O_2(a)$ or $O_2(X) + M$, together with the reactions $O_2(a) + O_2(a) \rightarrow O_2(a) + O_2(X)$ and $O_2(a) + O_2(a) \rightarrow O_2(X) + O_2(X)$, leads to the loss of $O_2(a)$ molecules. From the analysis of the data on the content of $O_2(a)$ at the output of the SOG, the authors of [25] obtained the total effective rate constant of all these three reactions, equal to $\sim 10^{16}$ cm^3, which is close to the value 8.2×10^{-17} cm^3 s^{-1} of [26]. Hence, in correspondence with these data, the channel (1) contributes nearly a half of the total loss of the singlet oxygen in the reaction $O_2(a) + O_2(a) \rightarrow$ products.

Thus, we obtained the dependence of the ratio of specific powers of the dimole radiation and the radiation in the band b–X of the singlet oxygen in the gas flow $O_2(X)-O_2(^1\Delta)-O_2(^1\Sigma)-H_2O-CO_2$ on the concentration of CO_2. This allowed us to determine the rate constant for the reaction $O_2(a) + O_2(a) \rightarrow O_2(b) + O_2(X)$ in the temperature range 320–340 K, that appeared to equal $(4.5\pm1.1)\times10^{-17}$ cm^3 s^{-1}. The rate constant obtained is nearly two times larger than those known from the literature [2, 6].

References

1. Slanger T.M., Copeland R.A. *Chem. Rev.*, **103**, 4731 (2003).
2. Derwent R.G., Thrush B.A. *Trans. Far. Soc.*, **67**, 2036 (1971).
3. Perram G.P. *Int. J.Chem. Kin.*, **27**, 817 (1995).
4. Heidner R.F., Gardner C.E., Segal G.I., El-Sayed T.M. *J. Phys. Chem.*, **87**, 2348 (1983).
5. Arnold S.J., Finlayson N., Ogryzlo E.A. *J. Chem. Phys.*, **44**, 2529 (1966).
6. Fisk G.A., Hays G.N. *J. Chem. Phys.*, **77**, 4965 (1982).
7. Lilenfeld H.V., Carr P.A.G., Hovis F.E. *J. Chem. Phys.*, **81**, 5730 (1984).
8. Heidner R.F., Gardner C.E., El-Sayed T.M., Segal G.I., Kasper J.V.V. *J. Chem. Phys.*, **74**, 5618 (1981).
9. Borrell P.M., Borrell P., Grant K.R., Pedley M.D. *J. Phys. Chem.*, **86**, 700 (1982).
10. Liu J., Morokuma K. *J. Chem. Phys*., **123**, 204319 (2005).
11. Lu R., Zhang P., Chu T., Xie T., Han. K. *J. Chem. Phys*., **126**, 124304 (2007).
12. Azyazov V.N., Zagidullin M.V., Nikolaev V.D., Svistun M.I., Khvatov N.A. *Kvantovaya Elektron.*, **22**, 443 (1995) [*Quantum Electron*., **25**, 418 (1995)].
13. Zagidullin M.V. *Opt. Spectrosk*., **109** (4), 538 (2010).
14. Falick A.M., Mahan B.H. *J. Chem. Phys.*, **47**, 4778 (1967).
15. Rothman L.S., Jacquemart D., Barbe A., et al. *J. Quant. Spec. Rad. Trans.*, **96**, 139 (2005).
16. Naus H., Ubachs W. *Appl. Opt.*, **38**, 3423 (1999).
17. Tiedje H.F., DeMille S., MacArtur L, Brooks R.L. *Can. J.Phys.*, **79**, 773 (2001).
18. Singh J.P., Setser D.W. *J. Phys. Chem.*, **89**, 5353 (1985).
19. Boodaghians R.B., Borrell P.M., Borrell P. *Chem. Phys. Lett.*, **97**, 193 (1983).

20. Muller D.F., Houston P.L. *J. Phys. Chem.*, **85**, 3563 (1981).
21. Choo K.Y., Leu M. *Int. J. Chem. Kinetics*, **17**, 1155 (1985).
22. Aviles R.G., Muller D.F., Houston P.L. *Appl. Phys. Lett.*, **37**, 358 (1980).
23. Azyazov V.N., Mikheev P., Postell D., Heaven M.C. *Chem. Phys. Lett.*, **482**, 56 (2009).
24. Long D.A., Havey D.K., Okumura M., Miller C.E., Hodges J.T. *J. Quant. Spec. Rad. Trans.*, **111**, 2021 (2010).
25. McDermott W.E., Hobbs K., Henshaw T. *Proc. SPIE Int. Soc. Opt. Eng.*, **7131**, 713112L-1 (2007).
26. Zagidullin M.V., Khvatov N.A. *Kvantovaya Elektron.*, **40**, 800 (2010) [*Quantum Electron.*, **40**, 800 (2010)].